



Full length article



## Exposure to concentrated ambient PM<sub>2.5</sub> (CAPM) induces intestinal disturbance via inflammation and alternation of gut microbiome

Shanshan Xie<sup>a,1</sup>, Caihong Zhang<sup>c,1</sup>, Jinzhuo Zhao<sup>b,\*</sup>, Dan Li<sup>a,d,\*</sup>, Jianmin Chen<sup>a</sup>

<sup>a</sup> Shanghai Key Laboratory of Atmospheric Particle Pollution and Prevention (LAP3), Department of Environmental Science and Engineering, Fudan University, Shanghai 200438, China

<sup>b</sup> Department of Environmental Health, School of Public Health and the Key Laboratory of Public Health Safety, Fudan University, Shanghai 200032, China

<sup>c</sup> Department of Obstetrics and Gynecology, Changhai Hospital, Second Military Medical University, Shanghai 200433, China

<sup>d</sup> IRDR International Center of Excellence on Risk Interconnectivity and Governance on Weather/Climate Extremes Impact and Public Health, Institute of Atmospheric Sciences, Fudan University, Shanghai, China

### ARTICLE INFO

Handling Editor: Adrian Covaci

#### Keywords:

Inhalation exposure  
Ambient PM<sub>2.5</sub>  
Inflammation  
Intestinal microbiome  
Correlations

### ABSTRACT

Air pollution causes a great disease burden worldwide. Recent evidences suggested that PM<sub>2.5</sub> contributes to intestinal disease. The objective of present study was to investigate the influence of ambient PM<sub>2.5</sub> on intestinal tissue and microbiome via whole-body inhalation exposure. The results showed that high levels and prolonged periods exposure to concentrated ambient PM<sub>2.5</sub> (CAPM) could destroy the mucous layer of the colon, and significantly alter the mRNA expression of tight junction (Occludin and ZO-1) and inflammation-related (IL-6, IL-10 and IL-1 $\beta$ ) genes in the colon, comparing with exposure to the filtered air (FA). The composition of intestinal microbiome at the phylum and genus levels also varied along with the exposure time and PM<sub>2.5</sub> levels. At the phylum level, Bacteroidetes was greatly decreased, while Proteobacteria was increased after exposure to CAPM, comparing with exposure to FA. At the genus level, *Clostridium XIVa*, *Akkermansia* and *Acetatifactor*, were significantly elevated exposure to CAPM, comparing with exposure to FA. Our results also indicated that high levels and prolonged periods exposure to CAPM altered metabolic functional pathways. The correlation analysis showed that the intestinal inflammation was related to the alteration of gut microbiome induced by CAPM exposure, which may be a potential mechanism that elucidates PM<sub>2.5</sub>-induced intestinal diseases. These results extend our knowledge on the toxicology and health effects of ambient PM<sub>2.5</sub>.

### 1. Introduction

Air pollution was regarded as the fourth most important risk factor for death globally (Murray et al., 2020). PM<sub>2.5</sub> (particles with diameters of  $\leq 2.5 \mu\text{m}$ ), a critical air pollutant, caused approximate 4.14 million deaths worldwide in 2019 (Murray et al., 2020). Although studies on the adverse effects of PM<sub>2.5</sub> have mostly focused on respiratory and cardiovascular systems (Tschofen et al., 2019; Williams et al., 2019), emerging evidences have revealed a link between ambient PM<sub>2.5</sub> exposure and intestinal diseases (Mutlu et al., 2018; Ananthakrishnan et al., 2018).

PM<sub>2.5</sub> can penetrate deeply inside the lung, and enter the blood stream, therefore travel throughout the whole body (Apte et al., 2015). Furthermore, the inhaled PM<sub>2.5</sub> can be quickly cleared from the lung

into the intestinal tract via mucociliary transport (Apte et al., 2015; Li et al., 2017). Additionally, PM<sub>2.5</sub> can also be directly digested through depositing into the food and water supply (Valacchi et al., 2020). It has been estimated that about  $10^{12}$ – $10^{14}$  particles were ingested per day by an adult consuming a typical western diet (Valacchi et al., 2020). Therefore, the intestinal tract and intestinal microbiome can contact a large amount of PM<sub>2.5</sub> through inhalation and direct ingestion (Li et al., 2017; WHO, 2021).

The intestinal microbiome is considered as a vital “organ” and plays critical roles in host health (Dang and Marsland, 2019). Increasing investigations have found that imbalances in the intestinal microbiome are associated with multiple diseases, including obesity, renal diseases, diabetes, allergies, and inflammatory bowel disease (IBD) (Delzenne et al., 2015). Previous researches have claimed that PM<sub>2.5</sub> and chemicals

\* Corresponding authors.

E-mail addresses: [jinzhuozhao@fudan.edu.cn](mailto:jinzhuozhao@fudan.edu.cn) (J. Zhao), [lidanfudan@fudan.edu.cn](mailto:lidanfudan@fudan.edu.cn) (D. Li).

<sup>1</sup> The authors contribute equally.

<https://doi.org/10.1016/j.envint.2022.107138>

Received 2 December 2021; Received in revised form 2 February 2022; Accepted 5 February 2022

Available online 14 February 2022

0160-4120/© 2022 The Authors.

Published by Elsevier Ltd.

This is an open access article under the CC BY-NC-ND license

(<http://creativecommons.org/licenses/by-nc-nd/4.0/>).

carried by the ambient PM<sub>2.5</sub> could change the mice intestinal microbiome by oral ingestion (Mutlu et al., 2011; Zhai et al., 2017). Recently, some studies also reported that inhalation of ambient PM<sub>2.5</sub> impacted gut microbiota (Ran et al., 2021; Wang et al. 2018). However, the influence of inhalable ambient PM<sub>2.5</sub> on intestinal inflammation and microbiota over different exposure duration is still unknown.

In the present study, we established filtered air (FA) and concentrated ambient PM<sub>2.5</sub> (CAPM) exposure chambers to simulate clear and heavily-polluted air conditions. Then, the C57BL/6J male mice were exposed in FA or CAPM chambers for 8, 16 and 24 weeks, respectively. The intestinal inflammation, the alteration of the gut microbiome, as well as their correlations, were systematically investigated after differential exposure periods, as well as the associated mechanisms.

## 2. Material and methods

### 2.1. Whole-body exposure in FA and CAPM chambers

This study employed 30 C57BL/6J male mice aged 3 weeks, which were supplied by the Animal Center of Shanghai Medical School, Fudan University in Shanghai, China. During the experimental period, all the mice were housed in a standard environment (temperature, 24 ± 2 °C; relative humidity, 60 ± 5%; 12:12 light–dark cycle). After 1 week of adjustable acclimation, 30 mice were randomly and medially divided into 6 groups (n = 5 mice each group): 8-week CAPM exposure, 16-week CAPM exposure, 24-week CAPM exposure, and the respective FA exposure controls. Then, the mice were consecutively exposed in the CAPM and FA chambers in the “Shanghai Meteorological and Environmental Animal Exposure System (Shanghai-METAS)” located in the Fudan University for 8, 16 or 24 weeks, respectively. The CAPM chamber is equipped with a versatile aerosol concentration enrichment system to generate CAPM, and the FA chamber is equipped with a high-efficiency particulate air filter (Geller et al., 2005). The real-time PM<sub>2.5</sub> concentrations in these two chambers were continuously determined by TEOM 1405 (Thermo, USA). The PM<sub>2.5</sub> in the FA and CAPM chambers,

as well as the ambient PM<sub>2.5</sub> in the air-conditioned animal-room, were collected by using Teflon filters. The elemental compositions were detected by inductively coupled plasma mass spectroscopy (ICP-MS), and PAHs were determined by high performance liquid chromatography (HPLC) as previously described (Wang et al. 2018; Ohura et al., 2005). The whole-body exposure in FA or CAPM chambers was carried out for 8 h/day and 6 days/week (except Sunday) from June to December 2018. After 8 h exposure every day, all mice were exposed to ambient air for another 16 h each day. All experimental procedures were carried out according to the Institutional Animal Care and Use Committees of Fudan University, and all the mice were treated humanely.

The experimental scheme is shown in Fig. 1A. After 8, 16 and 24 weeks of exposure in FA or CAPM chambers, each mouse was transferred to an autoclaved metabolism cage and allowed to defecate normally. Fecal samples from each mouse were collected and immediately transferred into a –80 °C freezer until processing. Then, the mice were decapitated, and the colon tissues were quickly dissected and put into RNAlater solution (Ambion, Life Technologies, CA, USA), which were transferred to a –80 °C freezer for further experiments.

### 2.2. Assessment of intestinal inflammation

Full-thickness sections of the colon were excised, immediately fixed in 4% paraformaldehyde solution, and embedded in paraffin. Thin sections (4 μm) were stained with hematoxylin-eosin (H&E), and the morphological characteristics were observed by using optical microscopy (Li et al., 2018). The colon pathological severity was estimated by independently scoring two parameters: edema and inflammatory cell infiltration. Grade 0: no abnormality; grade 1: lesions involving 25% of the colon; grade 2: lesions involving 25–50% of the colon; grade 3: lesions involving 50–75% of the colon; grade 4: lesions involving 75% or more of the colon. The total histopathological score was expressed as the total score of all parameters (Wolthuis et al., 2011).

The mRNA expression of tight junction protein-related genes (Occludin and zonula occludens (ZO)-1) and inflammation-related genes

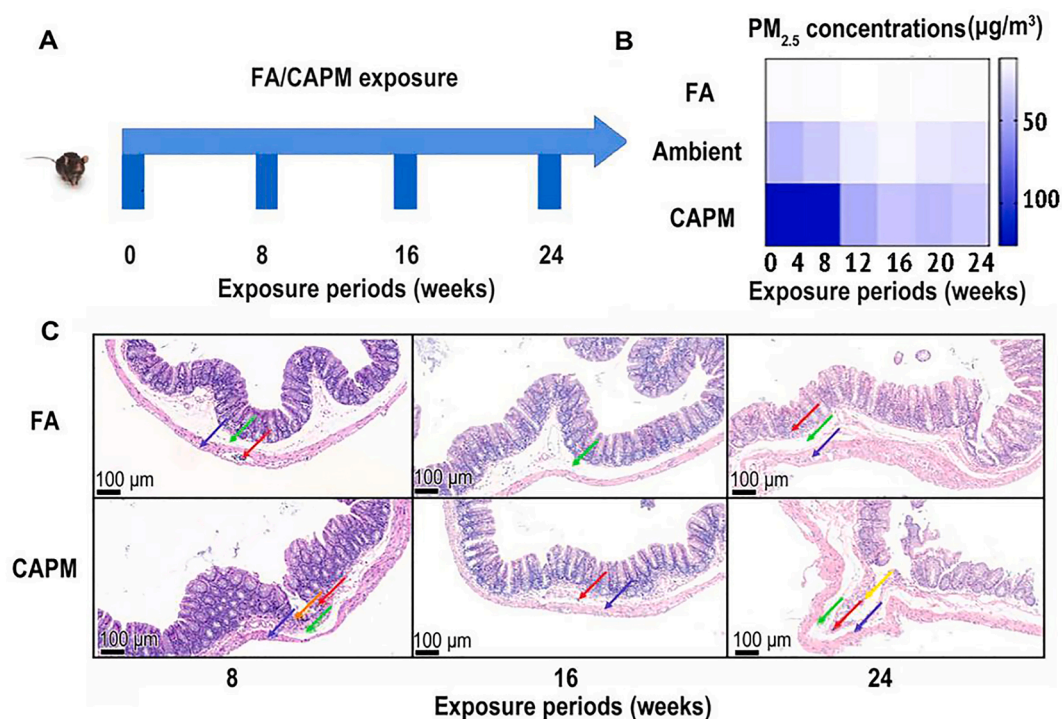


**Fig. 1.** Chronic exposure to CAPM results in gut inflammation. A. The experimental scheme; B. Exposure PM<sub>2.5</sub> concentration; C. H&E staining images of the colon in exposed mice. Magnification: ×10. Red arrow indicates inflammatory cells; purple arrow indicates vacuolation degeneration; green arrow indicates edema; yellow arrow indicates mucosal atrophy and necrosis. FA: filtered air; CAPM: concentrated ambient PM<sub>2.5</sub>. N = 5 in each group.

(IL-6, IL-10, IL-1 $\beta$ , TNF- $\alpha$ , IL-17A, IL-17F, and TRAF6) in colon tissue were determined, and the detailed information was described in Text S1 and Table S1.

### 2.3. The 16S rDNA sequencing

Total microbial genomic DNA from each fecal sample was extracted by using QIAamp DNA stool mini kits (Qiagen, Germany) following the manufacturer's instructions, and the DNA concentration was determined using a NanoDrop 2000 spectrophotometer (Thermo Fisher Scientific, USA) and the purity was detected on a 1% agarose gel. The qualifying DNA was amplified in the V4 region of the 16S rDNA gene through universal primers 515F (5'-GTGYCAGCCGGTAA-3') and 806R (5'-GACTACHVGGGGTATCTATCC-3') with dual-index barcodes. Sequencing was performed on the Illumina MiSeq platform at Micro-Analy company (Anhui, China).

### 2.4. Bioinformatics analysis

Processing of sequence reads were analyzed by QIIME (version 1.8.0). The raw reads with a lower quality score than 30 and short length than 200 bp were discarded. Pair-end reads that had a minimal overlap of 10 bp and a mismatched rate no more than 0.2 needed to be assembled. The repetitive reads were also discarded. The optimized reads were then clustered into operational taxonomic units (OTUs) with 97% read similarity by the average neighbor algorithm method in UCLUST and USEARCH software. The representative reads of OTUs were assigned to the SILVA database (<http://www.arb-silva.de>) on the QIIME platform to assess bacterial taxonomy at different levels. The OTU-based alpha diversities, including observed OTUs, Chao1, Shannon, and Simpson indexes, were calculated using Mothur (version 1.30). Principal component analysis (PCA) was determined based on using the relative abundances of OTUs. The linear discriminant analysis (LDA) coupled with the effect size (LefSe) method was used to identify the significant different bacterial taxa among groups (Zhou et al., 2021). As an emerging technique, the Phylogenetic Investigation of Communities by Reconstruction of Unobserved States 2 (PICRUSt2) analysis for metagenomes prediction has been widely applied (Li et al., 2018; Zhou et al., 2019). PICRUSt2 combined with the Kyoto Encyclopedia of Genes and Genomes (KEGG) database was employed to predict the metabolic function of bacterial communities in present study according to previous study (Zhou et al., 2019).

### 2.5. Statistical analysis

The data were analyzed with GraphPad Prism 7.0, and significance for all data tests was determined by the Kruskal – Wallis tests and corrected by the Bonferroni correction method.  $p$ -value < 0.05 was regarded as significant. The correlation between the composition of the intestinal microbiota and the relative mRNA expression of inflammation-related genes using Pearson correlation coefficient analysis using the R platform with the “psych” package.

## 3. Results and discussion

### 3.1. CAPM induced intestinal barrier injury and inflammation

The average PM<sub>2.5</sub> level in the FA chamber was  $12.85 \pm 1.82 \mu\text{g}/\text{m}^3$ , which was lower than the maximum 24-hour average concentrations of PM<sub>2.5</sub> ( $15 \mu\text{g}/\text{m}^3$ ) suggested by the World Health Organization (WHO) but higher than the annual concentrations of PM<sub>2.5</sub> level ( $5 \mu\text{g}/\text{m}^3$ ) suggested by the WHO (WHO, 2021). The average PM<sub>2.5</sub> levels in the CAPM chamber were  $124.79 \pm 103.73$ ,  $83.77 \pm 10.79$ , and  $68.55 \pm 23.85 \mu\text{g}/\text{m}^3$  during 0–8, 0–16 and 0–24 weeks (Fig. 1B and Table S2), respectively. The PM<sub>2.5</sub> levels in the CAPM chamber during all exposure duration were significantly higher than the 24-hour average

concentrations of PM<sub>2.5</sub> suggested by WHO ( $15 \mu\text{g}/\text{m}^3$ ) (WHO, 2021) and the grade I level of the Chinese Ambient Air Quality Standards ( $35 \mu\text{g}/\text{m}^3$ ) (Ministry of Environmental Protection of the People's Republic of China, 2012). The PM<sub>2.5</sub> levels in the CAPM chamber were commonly existed in areas with heavy air pollution in China and other regions worldwide (Liu et al., 2017; Shi et al., 2020). Table S3 showed that the organic and metals of PM<sub>2.5</sub> in the CAPM chamber and FA chamber was comparable to that of ambient PM<sub>2.5</sub>, suggesting that our exposure system didn't alter the chemical compositions of PM<sub>2.5</sub>.

The H&E staining of colon tissue showed that the structure of the mucous layer was significantly damaged in the CAPM-exposed groups, with the substratum of the mucous layer showing pathological changes, including focal atrophic necrosis of the mucosa (Fig. 1C). In contrast, FA-exposed mice exhibited slight focal atrophic necrosis of the mucosa after 24 weeks of exposure (Fig. 1C). Fig. S1 showed a significant increase in total histopathological score in CAPM-exposed mice (2.60) compared to FA-exposed mice (1.20) after 16-week exposure (FA-16 versus CAPM-16,  $p < 0.05$ ). The total histopathological score of CAPM-exposed mice (3.20) after 24-week exposure was significantly higher than that in FA-exposed mice (1.40) after 24-week exposure (FA-24 versus CAPM-24,  $p < 0.05$ ) (Fig. S1). These results suggested that high levels and prolonged periods of ambient PM<sub>2.5</sub> exposure could destroy the mucous layer of the colon and damage the intestinal barrier.

To further explore the influence of PM<sub>2.5</sub> on intestinal barrier integrity, we evaluated the mRNA expression of tight junction protein genes (Occludin and ZO-1) in the colon by using RT-qPCR. The expression levels of Occludin and ZO-1 were significantly lower in the CAPM-exposed mice than that of the FA-exposed mice after 8-week exposure (Fig. 2A and B), indicating that the acute exposure to CAPM lead to an increase in gut barrier permeability. Furthermore, the expression of Occludin and ZO-1 decreased along with the increasing of the exposure periods in both the FA- and CAPM-exposed groups (Fig. 2A and B). These results suggested that long-term exposure to relatively low level of PM<sub>2.5</sub> in FA chamber ( $12.85 \pm 1.82 \mu\text{g}/\text{m}^3$ ) also led to an increase in gut barrier permeability. Increasing epidemiological studies indicate that even low concentrations of PM<sub>2.5</sub> can still cause morbidity and mortality, contributing to the reduction of PM<sub>2.5</sub> guideline level suggested by the WHO (WHO, 2021; Di et al., 2017; Cakmak et al., 2018). Our result confirmed that long time exposure to relatively low levels of PM<sub>2.5</sub> ( $<15 \mu\text{g}/\text{m}^3$ ) were also harmful to health.

Increases in gut barrier permeability have been linked with intestinal inflammation (Al-kindi et al., 2020). The expression levels of inflammation-related genes (IL-6, IL-10, IL-1 $\beta$  and TNF- $\alpha$ ) were significantly up-regulated in the CAPM-exposed mice compared with the FA-exposed mice (Fig. 2C-F). However, the expressions of IL-17A, IL-17F and TRAF6 (Fig. 2G-I) were similar in these two groups. In particular, the expressions of IL-6 and IL-10 genes were positively correlated with the exposure periods in the CAPM groups, with  $R^2 = 0.78$  and  $0.77$ , respectively (Fig. S2). These results suggested that long-term exposure to CAPM can trigger accumulated inflammation in intestinal. Epidemiological data also showed that long-term exposure to air pollution had a significantly greater influence on mortality than short-term exposure (Al-kindi et al., 2020).

IL-10 is an anti-inflammatory cytokine produced by activated immune cells (Dutta et al., 2015). The mRNA expression of IL-10 in the CAPM-exposed group was 2.23-fold higher than that in the FA-exposed group after 24 weeks of exposure (Fig. 2D). Previous studies indicated that IL-10 could to be induced as a mechanism of feedback control under strong inflammatory stimulation (Anderson et al., 2007; McGeachy et al., 2007). Our results indicated that long-term exposure of CAPM induced gut inflammation, then induced anti-inflammation. The expression of IL-1 $\beta$  and TNF- $\alpha$  in the CAPM-exposed group were significantly higher than that in the FA-exposed group after 8 weeks of exposure (Fig. 2E), which may be due to the relatively high PM<sub>2.5</sub> concentrations in the CAPM chambers ( $124.97 \pm 103.73 \mu\text{g}/\text{m}^3$ ) during 0–8 weeks (Fig. 1B and Table S2). The increase of IL-1 $\beta$  induced the

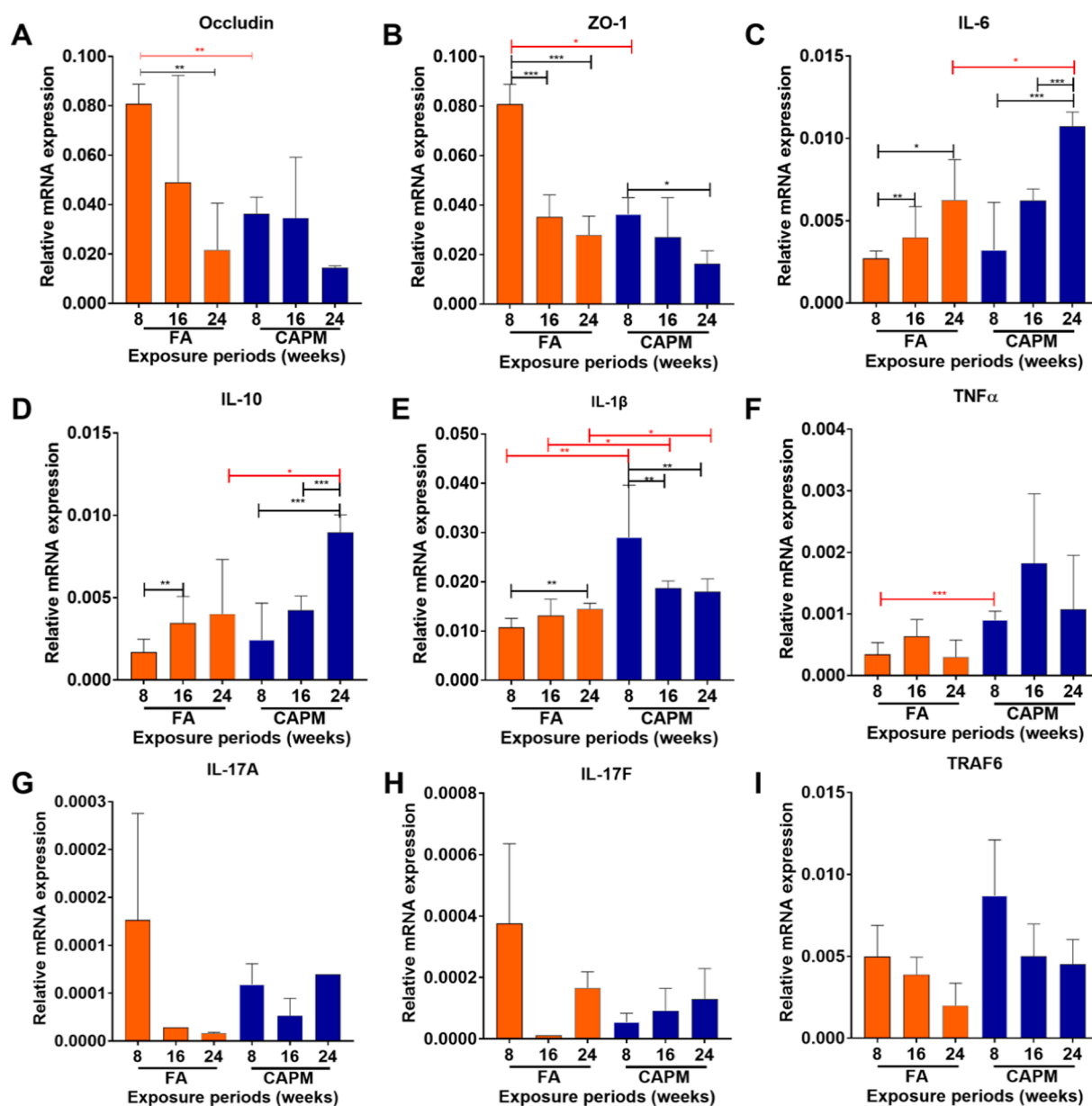


**Fig. 2.** Intestinal inflammation was evaluated by the relative mRNA expression of tight junction protein-related genes (Occludin and ZO-1) (A and B) and inflammation-related genes (IL-6, IL-10, IL-1 $\beta$ , TNF- $\alpha$ , IL-17A, IL-17F and TRAF6) in colon tissue (C-I). Values presented as fold change ( $2^{-\Delta\Delta CT}$ ) relative to the internal control gene GAPDH, and values are expressed as the mean  $\pm$  SD. Significant differences were analyzed by the Kruskal – Wallis tests and corrected by the Bonferroni correction method; \* $p < 0.05$ , \*\* $p < 0.01$ , and \*\*\* $p < 0.001$ . FA: filtered air; CAPM: concentrated ambient PM<sub>2.5</sub>. N = 5 in each group.

accumulation of macrophages, neutrophils and mast cells (Wang et al., 2017). Furthermore, the increases in IL-1 $\beta$  and TNF- $\alpha$  could trigger intestinal permeability, and they have been proven to be relevant with the pathogenesis of IBD (Zhu et al., 2016). These results suggest that acute exposure to CAPM influence the gut barrier permeability. In summary, long-term whole-body PM<sub>2.5</sub> exposure can alter epithelial permeability, increase gut inflammation, induce irrecoverable pathological changes, and therefore cause adverse health effects. Fig. S3 and Table S4 indicated that the exposure levels of Ni, Mn, Fe, Zn, Cu, and Cr carried by PM<sub>2.5</sub> during exposure periods were significantly positively correlated to the relative expression of inflammation related gene named IL-6 ( $r = 0.95, 0.95, 0.98, 0.98, 0.99$  and  $0.96$ , respectively;  $p < 0.05$ ). We also found that the exposure levels of Ni, Mn, Fe, Zn, Cu, and Cr carried by PM<sub>2.5</sub> during exposure periods had positive correlation with the relative expression of inflammation related gene named TNF $\alpha$  ( $r = 0.95, 0.96, 0.96, 0.97, 0.98$  and  $0.95$ , respectively;  $p < 0.05$ ). The exposure levels of

Benzo(b)fluoranthene, Naphthalene, Benzo(k)fluoranthene, and Dibenz(a,h)anthracene belonging to PAHs showed strong positive correlations with the relative expression of IL-1 $\beta$  ( $r = 0.86, 0.83, 0.95$  and  $0.85$ , respectively;  $p < 0.05$ ). These results may suggest that the change exposure levels of chemicals carried by PM<sub>2.5</sub> may be related to gut inflammation.

### 3.2. CAPM changed the intestinal microbiome

Through PCA analysis, we found that mice exposed for different periods tended to cluster separately, emphasizing that the age of mice significantly impacted the gut microbiome in both FA and CAPM chambers (Fig. 3A), which were consistent with the previous report (Zhang et al., 2018). Age-dependent alterations in the gut microbial composition are related to systemic inflammation and disease processes (Spychala et al., 2018).

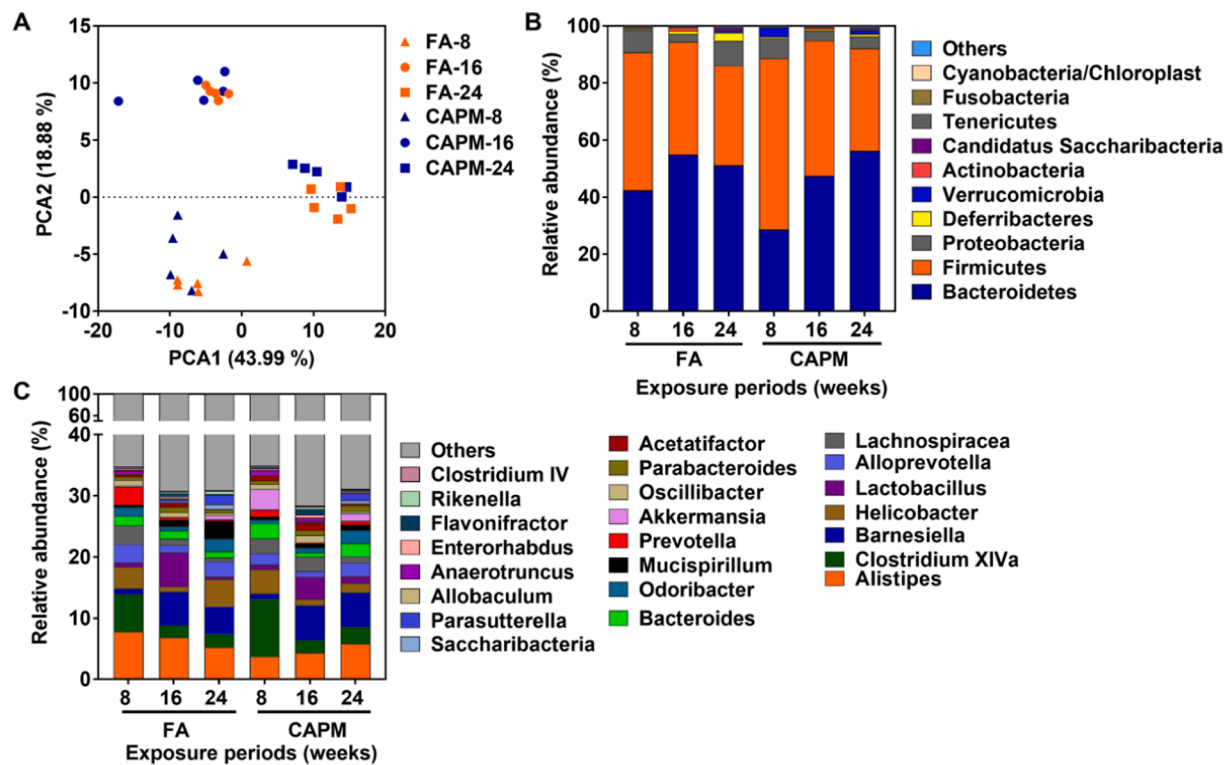


Fig. 3. Chronic exposure to CAPM triggers the alternations of gut microbiota compositions. A.PCA of all fecal samples using OTUs. B.Relative abundances of 10 most abundant phyla. C.Relative abundances of 23 most abundant genus. FA: filtered air; CAPM: concentrated ambient PM<sub>2.5</sub>. N = 5 in each group.

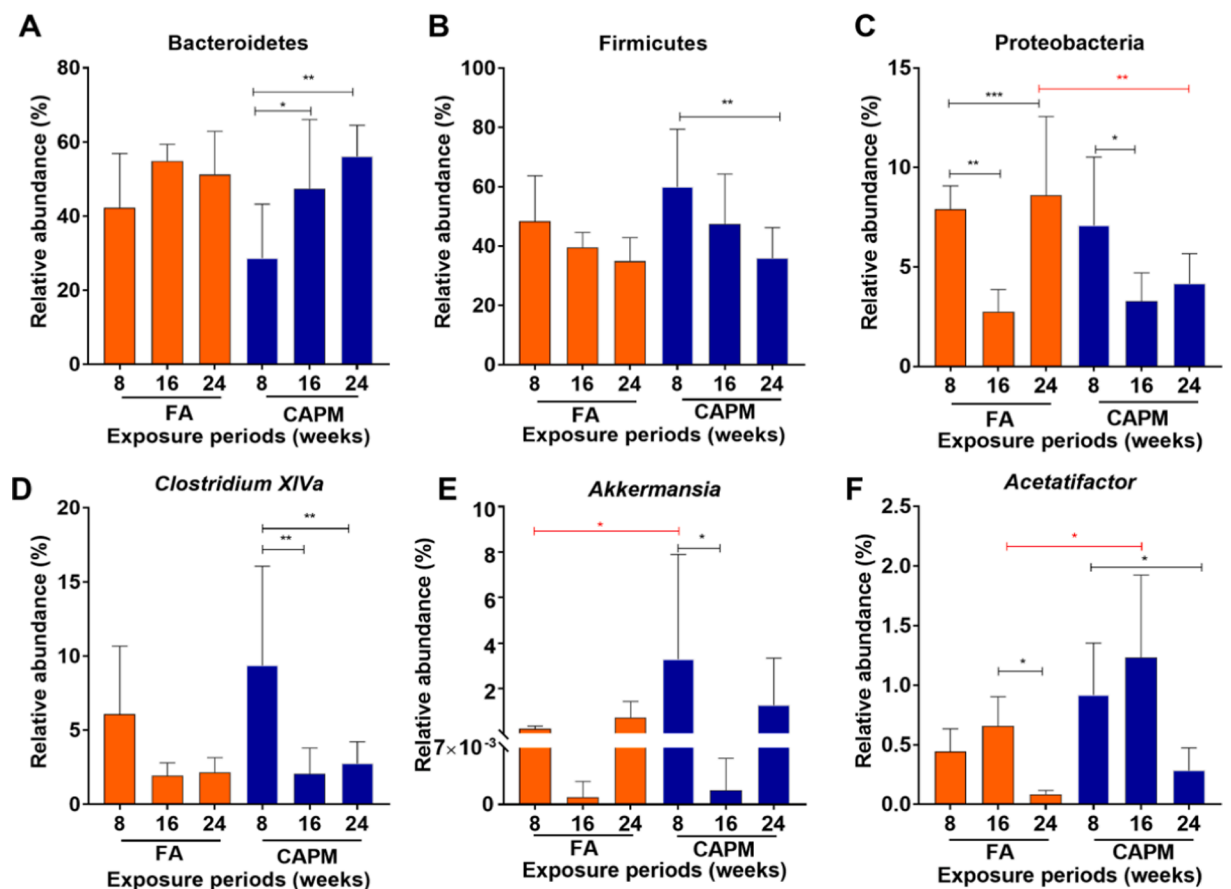


Fig. 4. Significant differences in phylum (A-C) and genera (D-F) composition were analyzed by the Kruskal – Wallis tests and corrected by the Bonferroni correction method; \* $p < 0.05$ , \*\* $p < 0.01$ , and \*\*\* $p < 0.001$ . FA: filtered air; CAPM: concentrated ambient PM<sub>2.5</sub>. N = 5 in each group.

After 8 weeks of exposure, the Bray-Curtis distances showed a significant difference between the FA- and CAPM-exposed groups (Fig. S4). The most important reason for this phenomenon is that the PM<sub>2.5</sub> levels in the CAPM chamber was relatively higher than that in the FA chamber during 0–8 weeks (Fig. 1B). However, these two groups tended to be similar after 16 and 24 weeks of exposure (Fig. 3A). Accordingly, the PM<sub>2.5</sub> levels in CAPM (38.12 ± 14.04 µg/m<sup>3</sup>) chamber were slightly higher than that in FA chamber during 16–24 weeks.

Even ambient PM<sub>2.5</sub> appeared to have no significant effect on the alpha diversity of gut microbiota (Fig. S5), the relative abundances of certain taxa at both phylum and genera levels varied in the FA- and CAPM-exposed groups (Figs. 3 and 4). The Firmicutes, Bacteroidetes and Proteobacteria phyla were the major phyla (98.80%) in the gut microbiota of the mice in both the FA and CAPM groups (Fig. 3B and Fig. 4A-C), which was consistent with previous studies (Wang et al., 2018; Du et al., 2020a). The relative abundances of Bacteroidetes in the CAPM-exposed groups were increased, while the relative abundances of Bacteroidetes were reduced along with exposure time (Fig. 4A). The relative abundance of Firmicutes in the CAPM-exposed groups were higher than that in the FA-exposed groups at the same exposure time (Fig. 4). After

24-week exposure, the relative abundance of Proteobacteria was significantly lower in CAPM-exposed groups than that in FA-exposed groups. The Firmicutes/Bacteroidetes ratio, an indicator of the imbalance of gut microbiota, was relatively higher in the CAPM-exposed groups than that of the FA-exposed groups after 8 weeks, which may also be attributed to the higher concentrations of PM<sub>2.5</sub> in the CAPM chamber during 0–8 weeks (Fig. S6). This ratio is associated with some diseases, such as obesity and type 2 diabetes (Han et al., 2018). Precious evidences also showed that PM is associated with obesity and impaired glucose metabolism (Gaio et al., 2019).

At the genus level, *Clostridium XIVa*, *Akkermansia* and *Acetatifactor*, belonging to the Bacteroidetes phylum, were higher in CAPM-exposed samples than that in FA-exposed samples (Fig. 3C and Fig. 4D-F). *Clostridium XIVa* is a butyrate producer, and related to anti-inflammatory processes and IBD (Zhou et al. 2018). The abundance of *Akkermansia* in the CAPM-exposed group was 13.94-fold higher than that in the FA-exposed group after 8 weeks exposure (Fig. 4D-F), which may be resulted from the relatively high PM<sub>2.5</sub> concentrations in the CAPM chambers (124.97 ± 103.73 µg/m<sup>3</sup>) during 0–8 weeks (Fig. 1B and Table S2). *Akkermansia*, a gram-negative strictly anaerobic probiotic, is

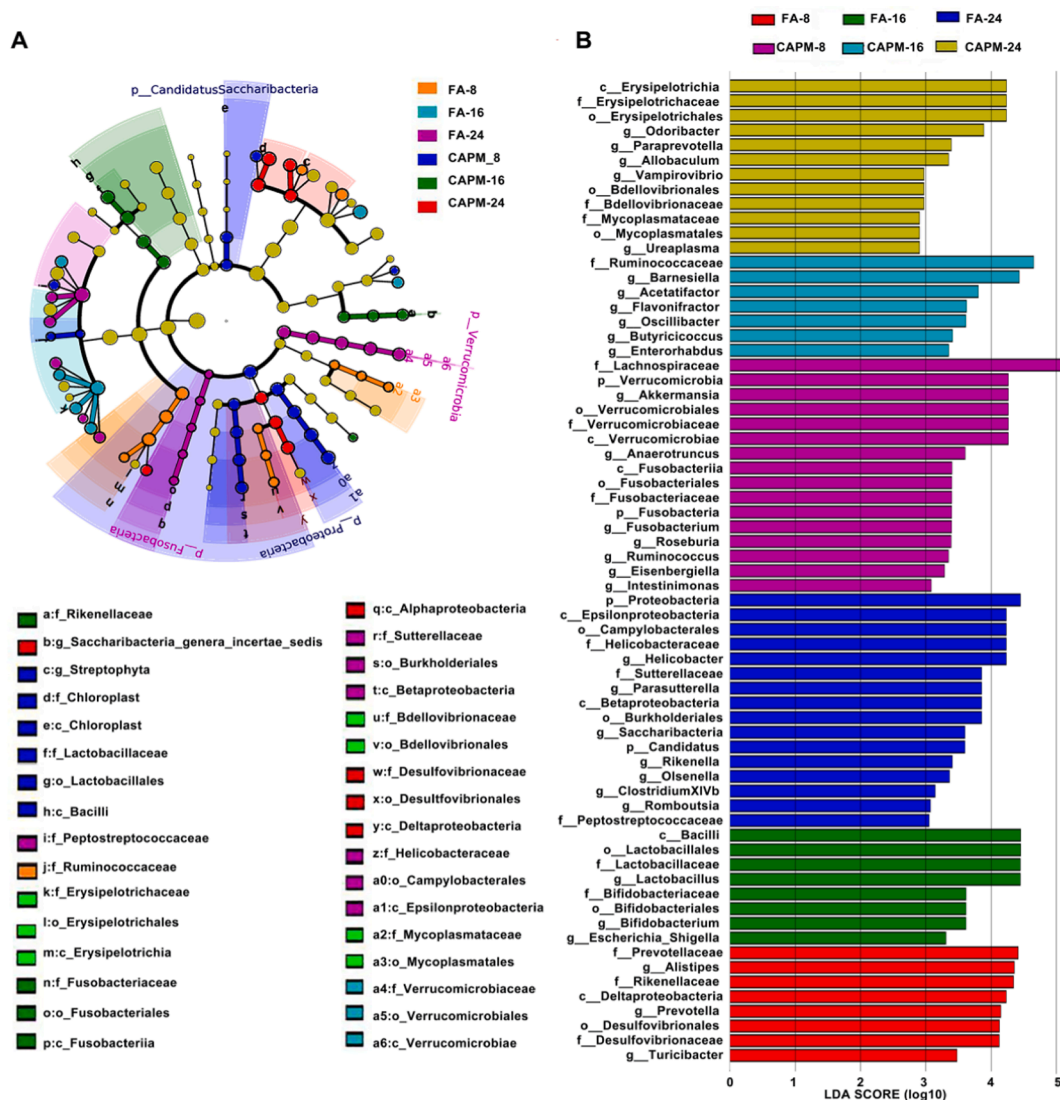


Fig. 5. Cladogram plot of the gut microbiota. A. Cladogram plotted to represent the microbial differences in FA-8, -16, -24, and CAPM-8, -16, -24 exposed mice groups. B. LefSe analysis shows differentially abundant bacterial groups as biomarkers determined using Kruskal–Wallis test ( $p < 0.05$ ) with LDA score of > 2.0. FA-8, -16, -24: mice exposed to the filtered air (FA) for 8, 16 and 24 weeks, respectively. CAPM-8, -16, -24: mice exposed to the concentrated ambient PM<sub>2.5</sub> (CAPM) for 8, 16 and 24 weeks. N = 5 in each group.

essential to the integrity of the mucous layer (Xie et al., 2019). Acute exposure to CAPM (8 weeks) altered the abundance of *Akkermansia*, which may lead to an increase in gut barrier permeability. After 24 weeks exposure of FA, the abundance of *Akkermansia* was 3.23-fold higher than that in FA group after 8 week-exposure (Fig. 4E). A previous study showed that *Akkermansia* has strong anti-inflammatory effects (Han et al., 2019). The abundance of *Akkermansia* was correlated with inflammatory status and glucose tolerance in the host (Xie et al., 2019). Our results suggested that long time exposure to low levels of PM<sub>2.5</sub> can induce the increase of *Akkermansia* and thus trigger inflammation.

We also conducted LEfSe and linear discriminant analysis (LDA) using the relative abundances of genus to find the differential microbial taxa between FA- and CAPM-exposed groups (Fig. 5). Specific bacterial genera, including *Akkermansia*, *Anaerotruncus*, *Fusobacterium*, *Roseburia*, *Ruminococcus*, *Eisenbergiella* and *Intestinimonas*, were found in the CAPM-exposed group after 8 weeks exposure (Fig. 5). The LDA scores were used to identify the greatest difference. High concentrations of PM<sub>2.5</sub> exposure in the CAPM chamber significantly changed the relative abundances of 16, 7, and 12 bacterial taxa after 8-, 16- and 24-week exposures, respectively (Fig. 5). Exposure to FA significantly increased the relative abundances of 8, 8, and 16 taxa of gut bacteria after 8-, 16- and 24-week exposures, respectively. These results demonstrated that long-term exposure to PM<sub>2.5</sub> induced gut microbiota dysbiosis, and might alter the metabolic processes. Fig. S7 and Table S5 showed that the exposure levels of certain PAHs, such as Acenaphthylene, Fluorene, Pyrene, Benzo(a)anthracene, Dibenz(a,h)anthracene, Benzo(k)

gluoranthene, Naphthalene, and Fluoranthene, were significantly associated with some phylum of gut microbiota. The exposure levels of Dibenz(a,h)anthracene, Benzo(k)gluoranthene, Naphthalene, and Fluoranthene showed significant positive correlations with the relative abundance of Verrucomicrobia ( $r = 0.96, 0.98, 0.87$  and  $0.92$ , respectively;  $p < 0.05$ ). A previous study indicated that the relative abundance of Verrucomicrobia was significantly positive related to total cholesterol, triglyceride, and high-density lipoprotein (Liu et al., 2020). Acenaphthylene and Fluorene showed a positively correlation with the relative abundance of Tenericutes ( $r = 0.82$  and  $0.82$ , respectively;  $p < 0.05$ ) (Fig.S7). A previous study found that Benzo(a)pyrene disturbs human gut homeostasis by impacting the volatile metabolome and transcriptome of gut microbiota (Defois et al., 2017). These results indicated that the change of the exposure levels of certain PAHs carried by PM<sub>2.5</sub> might perturb gut microbiota composition and influence the host health.

### 3.3. Correlations among intestinal inflammation and changes of gut microbiota

As showed in Fig. S8 and Fig. 6, there were strong correlations among the relative abundances of certain gut bacteria and the mRNA expression of genes involved in inflammation. The expression of the IL-6 and IL-10 genes positively correlated with *Parabacteroides* ( $r = 0.90, p < 0.05$ ;  $r = 0.90, p < 0.05$ ) (Fig. 6). The expressions of IL-17A ( $r = 0.92, p < 0.05$ ) and IL-17F ( $r = 0.82, p < 0.05$ ) were also positively related to the

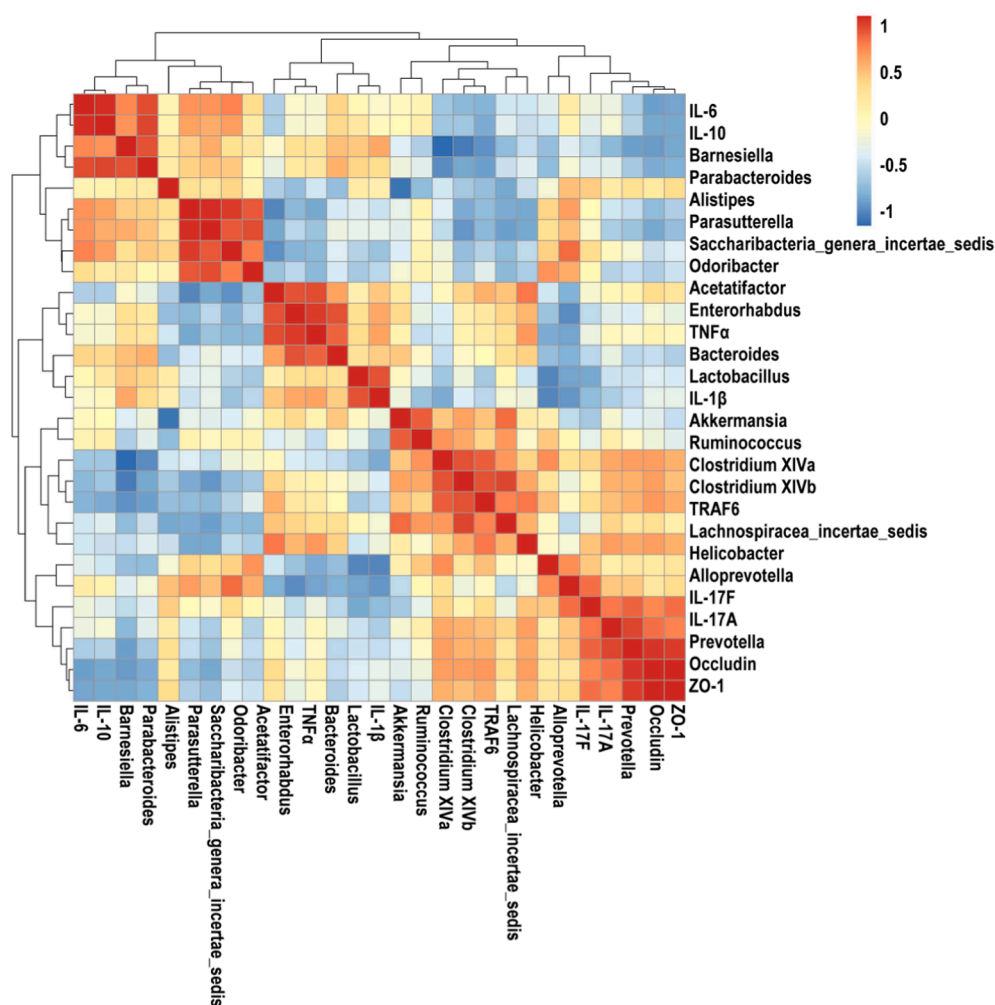


Fig. 6. The correlations among gut microbiota composition in genera and the relative mRNA expression of genes involved in inflammation and intestinal barrier. The color represents the correlation coefficient.  $N = 5$  in each group.

abundance of *Prevotella* (Fig. 6), which is related to lung inflammation (Waldman and Balskus, 2018). The expression of TRAF6 had positive correlations with the Firmicutes phylum ( $r = 0.91, p < 0.05$ ) and genus *Clostridium XIVa* ( $r = 0.91, p < 0.05$ ), but a negative correlation with the phylum Bacteroidetes ( $r = -0.84, p < 0.05$ ) (Fig. S5 and Fig. 6). Specifically, the mRNA expression of the IL-1 $\beta$  gene was strongly positively correlated with the phylum Verrucomicrobia ( $r = 0.88, p < 0.05$ ) and the genus *Akkermansia* ( $r = 0.83, p < 0.05$ ), while negatively correlated with the genus *Alistipes* ( $r = -0.92, p < 0.05$ ). A previous study also showed that *Akkermansia*, a representative Verrucomicrobia, had a strong positive correlation with gut inflammation (Han et al., 2019). Considering the higher relative abundance of *Akkermansia* in CAPM-exposed groups than in the FA-exposed group at the same exposure time, *Akkermansia* may exert proinflammatory effects in PM<sub>2.5</sub>-induced gut inflammation (Ganesh et al., 2013). The results indicated that there may be an interaction among the expression of inflammation- and intestinal barrier-related genes and key bacteria, which ultimately promotes gut injury.

### 3.4. Functional prediction of the gut microbiota

The total abundances of KEGG Orthology based on the KEGG pathways were reduced along with the exposure time in the FA and CAPM groups (Fig. S9). The results suggested that long-term exposure to PM<sub>2.5</sub> suppressed the metabolic activity of gut bacterial communities, indicating alternations in bacterial composition and diversity. PCA indicated that functional structure of samples in the different exposure periods were significantly distinguished, while the differences between FA- and CAPM-exposed groups at the same exposure time were not obvious (Fig. S10). Heatmap of top 20 functional pathways (hierarchy level 2) (Fig. S11) indicated that most of the top predicted pathways (such as glycan biosynthesis and metabolism, cell growth and death, metabolism of other amino acids, drug resistance, energy metabolism, lipid metabolism, folding, sorting and degradation, translation, replication and repair, metabolism of terpenoids and polyketides, nucleotide metabolism, membrane transport, protein families: genetic information processing, cellular community prokaryotes, carbohydrate metabolism, amino acid metabolism, and protein families: metabolism) were reduced along with the increasing exposure time in FA and CAPM groups. A previous study emphasized that the abundance of gut microbiota declined over time, and might be due to the increased complexity of gut microbiota along with time (Yatsunen et al., 2012). This study and ours implied that time influence the function of gut microbiota. The predicted functional pathways were also different between FA- and CAPM-exposed groups. Fig. S8 showed that the abundances of functional gene prediction (hierarchy level 2) of cell motility, membrane transport, signal transduction, carbohydrate metabolism, amino acid metabolism were enriched in CAPM-8 group compared to FA-8 group. Notably, amino acid metabolism pathway has been identified in the gut microbiota, and a previous study reported that it was impacted by PM<sub>2.5</sub> (Du et al., 2020b). Additionally, the findings on amino acid metabolism and carbohydrate metabolism pathways associated with Bacteroides were also supported by previous reports (Xiong et al., 2021; Chen et al., 2019). In our study, Bacteroides was decreased after 8-week CAPM exposure compared to that in the FA group (Fig. 2D), which may be the reason of amino acid metabolism enriched in CAPM-8 weeks group. Glycan biosynthesis and metabolism, metabolism of other amino acids, folding, sorting and degradation were declined in CAPM-exposed groups compared with FA-exposed groups at the same exposure time (8, 16, and 24 weeks), suggesting a reduction in the activity of gut microbiota communities under CAPM exposure. The alternations of gut microbial-mediated function is usually associated with host disease. Previous study showed that glycan biosynthesis and metabolism has been revealed to be related to arteriosclerosis formation (Hu et al., 2021). However, PICRUSt2 is only a way of predicting microbiota function; thus, further studies are required to investigate the accuracy of

microbiota function by metagenomic analysis.

## 4. Conclusions

In conclusion, long-term exposure to CAPM could damage the intestinal barrier, trigger intestinal inflammation, and change the intestinal microbial composition in mice. The composition of intestinal microbiome at the phylum and genus levels also varied along with the exposure time and PM<sub>2.5</sub> levels. High levels and prolonged periods exposure to CAPM also altered metabolic functional pathways. The correlation analysis suggested that intestinal inflammation might be related to certain intestinal bacteria, which may be a potential mechanism that explains inhalation PM<sub>2.5</sub>-induced inflammation in the intestine. In addition, the results of KEGG pathways analysis showed that exposure time markedly influenced the gut microbial functions. Some metabolic pathways were enriched after exposure to CAPM, and they might induce the metabolic diseases. The present results illuminated a new pathway for inhalation PM<sub>2.5</sub>-induced adverse health effects and associated mechanisms, which will contribute to the development of effective prevention.

## 5. Data availability statement

All data generated or analyzed during this study are included in this published article and its [supplementary information files](#).

## CRedit authorship contribution statement

**Dan Li and Jinzhuo Zhao:** Conceptualization, Methodology, Formal analysis, Software, Investigation, Writing - review & editing, Funding acquisition. **Shanshan Xie and Caihong Zhang:** Investigation, Formal analysis, Software, Data curation, Visualization, Writing - original draft. **Jianmin Chen:** Writing - review & editing, Funding acquisition.

## Declaration of Competing Interest

The authors declare that they have no known competing financial interests or personal relationships that could have appeared to influence the work reported in this paper.

## Acknowledgements

The content is solely the responsibility of the authors. This study was supported by the China National Natural Science Foundation (No. 22122601 and 92043301), the Open Research Fund Program of State Environmental Protection Key Laboratory of Food Chain Pollution Control (FC2021YB01) and Shanghai Natural Science Foundation (No. 20ZR1404300, 21DZ1202300 and 21230712800).

## Accession numbers

Raw sequence data in Fastq format have been deposited into the National Center for Biotechnology Information (NCBI) Sequence Read Archive (SRA) under BioProject PRJNA698299.

## Appendix A. Supplementary material

Supplementary data to this article can be found online at <https://doi.org/10.1016/j.envint.2022.107138>.

## References

- Al-Kindi, S.G., Brook, R.D., Biswal, S., Rajagopalan, S., 2020. Environmental determinants of cardiovascular disease: lessons learned from air pollution. *Nat. Rev. Cardiol.* <https://doi.org/10.1161/CIRCRESAHA.117.306458>.
- Ananthakrishnan, A.N., Bernstein, C.N., Iliopoulos, D., Macpherson, A., Neurath, M.F., Ali, R.A.R., Vavricka, S.R., Fiocchi, C., 2018. Environmental triggers in IBD: a review

- of progress and evidence. *Nat. Rev. Gastroenterol. Hepatol.* 15 (1), 39–49. <https://doi.org/10.1038/nrgastro.2017.136>.
- Anderson, C.F., Oukka, M., Kuchroo, V.J., Sacks, D., 2007. CD4(+)CD25(-)Foxp3(-) Th1 cells are the source of IL-10-mediated immune suppression in chronic cutaneous leishmaniasis. *J. Exp. Med.* 204 (2), 285–297. <https://doi.org/10.1084/jem.20061886>.
- Apte, J.S., Marshall, J.D., Cohen, A.J., Brauer, M., 2015. Addressing global mortality from ambient PM<sub>2.5</sub>. *Environ. Sci. Technol.* 49 (13), 8057–8066. <https://doi.org/10.1021/acs.est.5b01236>.
- Cakmak, S., Hebborn, C., Pinault, L., Lavigne, E., Vanos, J., Crouse, D.L., Tjepkema, M., 2018. Associations between long-term PM<sub>2.5</sub> and ozone exposure and mortality in the Canadian Census Health and Environment Cohort (CANHEC), by spatial synoptic classification zone. *Environ. Int.* 111, 200–211. <https://doi.org/10.1016/j.envint.2017.11.030>.
- Chen, R., Wang, J., Zhan, R., Zhang, L., Wang, X., 2019. Fecal metabolomics combined with 16S rRNA gene sequencing to analyze the changes of gut microbiota in rats with kidney-yang deficiency syndrome and the intervention effect of You-gui pill. *J. Ethnopharmacol.* 244, 112139. <https://doi.org/10.1016/j.jep.2019.112139>.
- Dang, A.T., Marsland, B.J., 2019. Microbes, metabolites, and the gut-lung axis. *Mucosal Immunol.* 12 (4), 843–850. <https://doi.org/10.1038/s41385-019-0160-6>.
- Defois, C., Ratel, J., Denis, S., Batut, B., Beugnot, R., Peyretailade, E., Engel, E., Peyret, P., 2017. Environmental Pollutant Benzo(a)Pyrene Impacts the Volatile Metabolome and Transcriptome of the Human Gut Microbiota. *Front. Microbiol.* 8.
- Delzenne, N.M., Cani, P.D., Everard, A., Neyrinck, A.M., Bindels, L.B., 2015. Gut microorganisms as promising targets for the management of type 2 diabetes. *Diabetologia.* 58 (10), 2206–2217. <https://doi.org/10.1007/s00125-015-3712-7>.
- Di, Q.; Dominici, F.; Schwartz, J. D. Air Pollution and Mortality in the Medicare Population REPLY. *N. Engl. J. Med.* 2017, 377, (15), 1498-1499, DOI: 10.1056/NEJMoa1702747.
- Du, H.P., Zhao, A.Q., Wang, Q., Yang, X.B., Ren, D.Y., 2020a. Supplementation of inulin with various degree of polymerization ameliorates liver injury and gut microbiota dysbiosis in high fat-fed obese mice. *J. Agr. Food. Chemj.* 68 (3), 779–787. <https://doi.org/10.1021/acs.jafc.9b06571>.
- Du, X., Zeng, X., Pan, K., Zhang, J., Song, L., Zhou, J.i., Chen, R., Xie, Y., Sun, Q., Zhao, J., Kan, H., 2020b. Metabolomics analysis of urine from healthy wild type mice exposed to ambient PM<sub>2.5</sub>. *Sci. Total Environ.* 714, 136790. <https://doi.org/10.1016/j.scitotenv.2020.136790>.
- Dutta, A., Huang, C.-T., Chen, T.-C., Lin, C.-Y., Chiu, C.-H., Lin, Y.-C., Chang, C.-S., He, Y.-C., 2015. IL-10 inhibits neuraminidase-activated TGF-beta and facilitates Th1 phenotype during early phase of infection. *Nat. Commun.* 6. <https://doi.org/10.1038/ncomms7374>.
- Gaio, V., Roquette, R., Dias, C.M., Nunes, B., 2019. Ambient air pollution and lipid profile: systematic review and meta-analysis. *Environ. Pollut.* 254, 113036. <https://doi.org/10.1016/j.envpol.2019.113036>.
- Ganesh, B.P., Klopffleisch, R., Loh, G., Blaut, M., Ryffel, B., 2013. Commensal *Akkermansia muciniphila* Exacerbates Gut Inflammation in *Salmonella* Typhimurium-Infected Gnotobiotic Mice. *Plos One.* 8 (9), e74963.
- Geller, M.D., Biswas, S., Fine, P.A., Sioutas, C., 2005. A new compact aerosol concentrator for use in conjunction with low flow-rate continuous aerosol instrumentation. *J. Aerosol Sci.* 36 (8), 1006–1022.
- Han, F., Wang, Y., Han, Y.Y., Zhao, J.X., Han, F.L., Song, G., Jiang, P., Miao, H.J., 2018. Effects of whole-grain rice and wheat on composition of gut microbiota and short-chain fatty acids in rats. *J. Agr. Food. Chemj.* 66 (25), 6326–6335. <https://doi.org/10.1021/acs.jafc.8b01891>.
- Han, Y.H., Song, M.Y., Gu, M., Ren, D.Y., Zhu, X.A., Cao, X.Q., Li, F., Wang, W.C., Cai, X. K., Yuan, B., Goulette, T., Zhang, G.D., Xiao, H., 2019. Dietary intake of whole strawberry inhibited colonic inflammation in dextran-sulfate-sodium-treated mice via restoring immune homeostasis and alleviating gut microbiota dysbiosis. *J. Agr. Food. Chemj.* 67 (33), 9168–9177. <https://doi.org/10.1021/acs.jafc.8b05581>.
- Hu, C., Wang, P., Yang, Y., Li, J., Jiao, X., Yu, H., Wei, Y., Li, J., Qin, Y., 2021. Chronic Intermittent Hypoxia Participates in the Pathogenesis of Atherosclerosis and Perturbs the Formation of Intestinal Microbiota. *Front. Cell. Infect. Micro.* 2021, 11, DOI:10.3389/fcimb.2021.560201.
- Li, R.S.; Yang, J.P., Saffari, A., Jacobs, J., Baek, K.I., Hough, G., Larauche, M.H., Ma, J.G., Jen, N., Moussaoui, N., Zhou, B., Kang, H., Reddy, S., Henning, S.M., Campen, M.J., Piseigna, J., Li, Z.P., Fogelman, A.M., Sioutas, C., Navab, M., Hsiai, T.K., 2017. Ambient Ultrafine Particle Ingestion Alters Gut Microbiota in Association with Increased Atherogenic Lipid Metabolites. *Sci. Rep.* 2017, 7, DOI:10.1038/srep42906.
- Li, Y., Liu, T., Yan, C., Xie, R., Guo, Z., Wang, S., Zhang, Y., Li, Z., Wang, B., Cao, H., 2018. Diammonium glycyrrhizinate protects against nonalcoholic fatty liver disease in mice through modulation of gut microbiota and restoration of intestinal barrier. *Mol. Pharmaceut.* 15 (9), 3860–3870.
- Liu, M., Huang, Y., Ma, Z., Jin, Z., Liu, X., Wang, H., Liu, Y., Wang, J., Jantunen, M., Bi, J., Kinney, P.L., 2017. Spatial and temporal trends in the mortality burden of air pollution in China: 2004–2012. *Environ. Int.* 2017, 98, 75–81. DOI:10.1016/j.envint.2016.10.003.
- Liu, Q., Li, Y., Song, X., Wang, J., He, Z., Zhu, J., Chen, H., Yuan, J., Zhang, X., Jiang, H., Zhang, S., Ruan, B., 2020. Both gut microbiota and cytokines act to atherosclerosis in ApoE<sup>-/-</sup> mice. *Microb. Pathog.* 138, 103827. <https://doi.org/10.1016/j.micpath.2019.103827>.
- McGeachy, M.J., Bak-Jensen, K.S., Chen, Y., Tato, C.M., Blumenschein, W., McClanahan, T., Cua, D.J., 2007. TGF-beta and IL-6 drive the production of IL-17 and IL-10 by T cells and restrain TH-17 cell-mediated pathology. *Nat. Immunol.* 8 (12), 1390–1397. <https://doi.org/10.1038/nri1539>.
- Murray, C.J.L., Aravkin, A.Y., Zheng, P., Abbafati, C., Abbas, K.M., 2020. Global burden of 87 risk factors in 204 countries and territories, 1990–2019: a systematic analysis for the Global Burden of Disease Study 2019. *Lancet.* 2020, 396 (10258) 1223–1249, DOI:10.1016/S0140-6736(20)30752-2.
- Mutlu, E.A., Comba, I.Y., Cho, T., Engen, P.A., Yazici, C., Soberanes, S., Hamanaka, R.B., Nigdelioglu, R., Meliton, A.Y., Ghio, A.J., Budinger, G.R.S., Mutlu, G.M., 2018. Inhalational exposure to particulate matter air pollution alters the composition of the gut microbiome. *Environ. Pollut.* 240, 817–830. <https://doi.org/10.1016/j.envpol.2018.04.130>.
- Mutlu, E.A., Engen, P.A., Soberanes, S., Urich, D., Forsyth, C.B., Nigdelioglu, R., Chiarella, S.E., Radigan, K.A., Gonzalez, A., Jakate, S., Keshavarzian, A., Budinger, G.R.S., Mutlu, G.M., 2011. Particulate matter air pollution causes oxidant-mediated increase in gut permeability in mice. *Part. Fiber. Toxicol.* 8 <https://doi.org/10.1186/1743-8977-8-19>.
- Ohura, T., Noda, T., Amagai, T., Fusaya, M., 2005. Prediction of personal exposure to PM<sub>2.5</sub> and carcinogenic polycyclic aromatic hydrocarbons by their concentrations in residential microenvironments. *Environ. Sci. Technol.* 39, 5599.
- Ran, Z., An, Y., Zhou, J.i., Yang, J., Zhang, Y., Yang, J., Wang, L., Li, X., Lu, D., Zhong, J., Song, H., Qin, X., Li, R., 2021. Subchronic exposure to concentrated ambient PM<sub>2.5</sub> perturbs gut and lung microbiota as well as metabolic profiles in mice. *Environ. Pollut.* 272, 115987. <https://doi.org/10.1016/j.envpol.2020.115987>.
- Shi, C., Nduka, I.C., Yang, Y., Huang, Y., Yao, R., Zhang, H., He, B., Xie, C., Wang, Z., Yim, S.H.L., 2020. Characteristics and meteorological mechanisms of transboundary air pollution in a persistent heavy PM<sub>2.5</sub> pollution episode in Central-East China. *Atmos. Environ.* 223, 117239. <https://doi.org/10.1016/j.atmosenv.2019.117239>.
- Spychala, M.S., Venna, V.R., Jandzinski, M., Doran, S.J., Durgan, D.J., Ganesh, B.P., Ajami, N.J., Putluri, N., Graf, J., Bryan, R.M., McCullough, L.D., 2018. Age-related changes in the gut microbiota influence systemic inflammation and stroke outcome. *Ann. Neurol.* 84 (1), 23–36. <https://doi.org/10.1002/ana.25250>.
- Tschofen, P., Azevedo, I.L., Muller, N.Z., 2019. Fine particulate matter damages and value added in the US economy. *P. Natl. Acad. Sci. USA* 116 (40), 19857–19862. <https://doi.org/10.1073/pnas.1905030116>.
- Valacchi, G., Magnani, N., Woodby, B., Maria Ferreira, S., Evelson, P., 2020. Particulate matter induces tissue oxinflammation: from mechanism to damage. *Antioxid. Redox Sign.* 33 (4), 308–1236. <https://doi.org/10.1089/ars.2019.8015>.
- Waldman, A.J., Balskus, E.P., 2018. The human microbiota, infectious disease, and global health challenges and opportunities. *ACS Infect. Dis.* 4 (1), 14–26. <https://doi.org/10.1021/acscinf.7b00232>.
- Wang, H.T., Song, L.Y., Ju, W.H., Wang, X.G., Dong, L., Zhang, Y.N., Ya, P., Yang, C., Li, F.S., 2017. The acute airway inflammation induced by PM<sub>2.5</sub> exposure and the treatment of essential oils in Balb/c mice. *Sci. Rep.* 2017, 7, DOI:10.1038/srep44256.
- Wang, W., Zhou, J., Chen, M., Huang, X., Xie, X., Li, W., Cao, Q., Kan, H., Xu, Y., Ying, Z., 2018. Exposure to concentrated ambient PM<sub>2.5</sub> alters the composition of gut microbiota in a murine model. *Part. Fiber. Toxicol.* 2018, 15, DOI:10.1186/s12989-018-0252-6.
- Williams, A.M., Phaneuf, D.J., Barrett, M.A., Su, J.G., 2019. Short-term impact of PM<sub>2.5</sub> on contemporaneous asthma medication use: Behavior and the value of pollution reductions. *P. Natl. Acad. Sci. USA* 116 (12), 5246–5253. <https://doi.org/10.1073/pnas.1805647115>.
- Wolthuis, E.K., Vlaar, A.P.J., Hofstra, J.-J., Roelofs, J.J.T.H., de Waard, V., Juffermans, N.P., Schultz, M.J., 2011. Plasminogen activator inhibitor-type I gene deficient mice show reduced influx of neutrophils in ventilator-induced lung injury. *Crit. Care Res. Pract* 2011, 1–11. <https://doi.org/10.1155/2011/217896>.
- Xie, M., Chen, G., Wan, P., Dai, Z., Zeng, X., Sun, Y.i., 2019. Effects of Dicafeoylquinic Acids from *Ilex kudingcha* on Lipid Metabolism and Intestinal Microbiota in High-Fat-Diet-Fed Mice. *J. Agr. Food. Chemj.* 67 (1), 171–183. <https://doi.org/10.1021/acs.jafc.8b05444.10.1021/acs.jafc.8b05444.s001>.
- Xiong, L.-L., Xue, L.-L., Chen, Y.-J., Du, R.-L., Wang, Q., Wen, S., Zhou, L., Liu, T., Wang, T.-H., Yu, C.-Y., 2021. Proteomics study on the cerebrospinal fluid of patients with encephalitis. *ACS Omega* 6 (25), 16288–16296. <https://doi.org/10.1021/acsomega.1c00367>.
- Yatsunenko, T., Rey, F.E., Manary, M.J., Trehan, I., Dominguez-Bello, M.G., Contreras, M., Magris, M., Hidalgo, G., Baldassano, R.N., Anokhin, A.P., Heath, A.C., Warner, B., Reeder, J., Kuczynski, J., Caporaso, J.G., Lozupone, C.A., Lauber, C., Clemente, J.C., Knights, D., Knight, R., Gordon, J.I., 2012. Human gut microbiome viewed across age and geography. *Nature* 486 (7402), 222–227. <https://doi.org/10.1038/nature11053>.
- Zhai, Q., Li, T., Yu, L., Xiao, Y., Feng, S., Wu, J., Zhao, J., Zhang, H., Chen, W., 2017. Effects of subchronic oral toxic metal exposure on the intestinal microbiota of mice. *Sci. Bull.* 62 (12), 831–840. <https://doi.org/10.1016/j.scib.2017.01.031>.
- Zhang, D.J., Han, J.J., Li, Y.Y., Yuan, B., Zho, J., Cheong, L.Z., Li, Y., Lu, C.Y., Su, X.R., 2018. Tuna oil alleviates D-galactose induced aging in mice accompanied by modulating gut microbiota and brain protein expression. *J. Agr. Food. Chemj.* 66 (22), 5510–5520. <https://doi.org/10.1021/acs.jafc.8b00446>.
- Zhou, L., Chen, C., Xie, J., Xu, C., Zhao, Q., Qin, J.G., Chen, L., Li, E., 2019. Intestinal bacterial signatures of the “cotton shrimp-like” disease explain the change of growth performance and immune responses in Pacific white shrimp (*Litopenaeus vannamei*). *Fish. Shellfish. Immunol.* 92, 629–636. <https://doi.org/10.1016/j.fsi.2019.06.054>.
- Zhou, Q., Xue, B., Gu, R., Li, P., Gu, Q., 2021. *Lactobacillus plantarum* ZJ316 attenuates helicobacter pylori-induced gastritis in C57BL/6 mice. *J. Agric. Food Chem.* 69 (23), 6510–6523. <https://doi.org/10.1021/acs.jafc.1c01070>.
- Zhou, W., Yan, Y., Mi, J., Zhang, H., Lu, L.u., Luo, Q., Li, X., Zeng, X., Cao, Y., 2018. Simulated digestion and fermentation in vitro by human gut microbiota of polysaccharides from bee collected pollen of Chinese wolfberry. *J. Agr. Food. Chemj.* 66 (4), 898–907. <https://doi.org/10.1021/acs.jafc.7b05546>.

Zhu, C.H., Ling, Q.J., Cai, Z.H., Wang, Y., Zhang, Y.B., Hoffmann, P.R., Zheng, W.J., Zhou, T.H., Huang, Z., 2016. Selenium-containing phycocyanin from se-enriched spirulina platensis reduces inflammation in dextran sulfate sodium-induced colitis by inhibiting NF-kappa B activation. *J. Agr. Food. Chemj.* 64 (24), 5060–5070. <https://doi.org/10.1021/acs.jafc.6b01308>.

Ministry of Environmental Protection of the People's Republic of China. (2012) Ambient Air Quality Standards (GB3095-2012).

WHO, 2021. World Health Organization (WHO) Global Air Quality Guidelines: Particulate Matter (PM<sub>2.5</sub> and PM<sub>10</sub>), Ozone, Nitrogen Dioxide, Sulfur Dioxide and Carbon Monoxide.